

Oversights in Characterising Heralded Single Photon Sources

Hugh Barrett^{1,2,*}, Imad I. Faruque²

¹*Quantum Engineering Centre for Doctoral Training,
Centre for Nanoscience and Quantum Information,
University of Bristol, Tyndall Avenue,
Bristol BS8 1FD, United Kingdom*

²*Quantum Engineering Technology Labs,
Centre for Nanoscience and Quantum Information,
University of Bristol, Tyndall Avenue,
Bristol BS8 1FD, United Kingdom*

**hugh.barrett@bristol.ac.uk*

(Dated: October 14, 2024)

The development of ideal sources is a fundamental challenge for the practical implementation of integrated photonic technologies for quantum applications. In this paper we analyse the state-of-the-art in heralded single photon sources; pointing out inconsistencies in the how key parameters, such as brightness and heralding efficiency, are characterised. We then suggest considerations that could be made to facilitate fairer comparison between literature results.

I. INTRODUCTION

Photons are a promising resource for emerging quantum technologies [1], with recent interest in applications such as information processing [2, 3], communications [4, 5], and demonstrations of fundamental physics [6, 7]. Integrated photonics in particular has risen as a promising candidate for practical and scalable [8] applications owing to their simplicity, small physical dimensions, and stability [9]. Silicon is often the platform of choice due to its abundance and compatibility with CMOS technologies [10]. The well-established silicon electronics industry has allowed for silicon integrated photonics to quickly become mass-manufacturable [11], and near-term applications are looking more likely.

One of the most significant roadblocks to using silicon integrated photonics for these applications is the development of ideal components, such as single photon sources [21]. The ideal single photon source emits deterministically, which is a great challenge across all platforms. While this continues to be a barrier to the development of, for example, quantum dot sources [22]; integrated photonics has a much clearer path towards deterministic single photon generation through multiplexing heralded single photon sources (HSPSs) [23].

HSPSs are also one of the best sources for generating indistinguishable photons which, as a result of the DiVincenzo criteria, is a key requirement for the high-visibility quantum interference required in

linear optical quantum computing [24]. Indistinguishable photons are required to perform operations and transmit information with minimal uncertainty, with ideal indistinguishability requiring ideal source purities [25, 26]. As a result, efforts to improve the purity of HSPSs have been explored widely in the literature [27–32].

The brightness and heralding efficiency of HSPSs have seen comparatively far less attention in the literature; and, while they are not fundamental requirements for indistinguishable sources, they are an important practical consideration for the scalability of sources. Improving both parameters enables faster information processing [23, 33], which is useful for scenarios that require a higher rate of computation protocols [34] or communications over high-loss channels [35]. Higher heralding efficiency gives lower key error rates in quantum key distribution [36], while high brightness single photon sources would be particularly useful for space-based quantum applications [37].

Studies on these free space communications applications have thus far have been constrained to bulk optical set-ups [38]. Integrated technologies have the potential to achieve an equivalent brightness to bulk optics, but with a smaller physical size [20]. However, currently the literature reports relatively low integrated source brightness values due to significant losses. This loss is in part due to parasitic processes such as two-photon absorption (TPA) and the use of high-loss grating couplers; although low-

Reference	Source	CAR	Spectral Purity (%)	Photon Number Purity (%)	Corrected Heralding Efficiency (%)	Effective Brightness (MHz mW ⁻²)
[12] ^{a,b}	MRR	≈ 10	85.5 ± 0.8	-	50	204
[13] ^{b,c}	MRR	352 ± 14	-	-	50	-
[14] ^{b,c}	MRR	≈ 35	-	-	50	-
[15] ^{b,c}	MRR	12105	-	99.5	50	149 ± 6
[16] ^d	ICR	1644 ± 263	99.1 ± 0.1	99.71 ± 0.21	93.1 ± 3.1	4.4 ± 0.1
[17]	ICR	81	99.1	-	52.4 ± 3.0	-
[18]	Multi-Mode Waveguide	-	99.04 ± 0.06	94.7 ± 0.1	91.0 ± 9.0	0.89
[19]	Microdisk	1386 ± 278	-	-	-	-

TABLE I: A comparison between the parameters of various literature HSPSs. Dashes represent when a particular parameter was not discussed.

^a Effective brightness was determined using a theoretical model.

^b Assuming maximum heralding efficiency at critical coupling.

^c A continuous-wave (CW) laser was used, so it is not possible to assume the maximum spectral purity that can be achieved by typical MRR (91.7%) [20].

^d Heralding efficiency is the average of separate signal and idler heralding efficiencies 92.1 ± 3.2 % and 94.0 ± 2.9% respectively.

loss couplers have been developed [39] and there are possible avenues to reduce the effects of TPA [40].

In this paper we will present two roadblocks to the advancement of high brightness or high heralding efficiency sources: the trade-offs between source parameters, and issues with the definitions of parameters that prevents fair comparison between sources. The comparisons made in this paper will be restricted to only silicon platforms, although the oversights raised are valid across all material platforms. We will also only consider photon pair generation through spontaneous four-wave mixing (SFWM), as SFWM is much easier to implement experimentally on-chip than other nonlinear processes, such as spontaneous parametric down-conversion (SPDC) which requires additional wavelength considerations to be made when designing the photonic chips [41].

II. LITERATURE OVERVIEW

Table I compares some of the highest values reported in the literature for some fundamental parameters of HSPSs, with a variety of different source architectures considered. All of these sources exhibit an coincidence-to-accidental ratio (CAR) greater than 10, the threshold for the ability to practically resolve coincidence events [14], so they can all be considered feasible for practical applications. The interferometrically coupled resonator

(ICR) structure discussed in [16] demonstrates the highest spectral purity (joint with the other ICR structure discussed in [17]), photon number purity, and corrected heralding efficiency of all of the sources in the table.

However, this ICR structure has a relatively low effective brightness compared to other sources. The highest claimed effective brightness is from the MRR structure in [12], although this is at the cost of the lowest spectral purity. This effective brightness value was determined using a theoretical model and it has been reported that experimental brightness measurements are often far below theoretical predictions [42].

When considering the parameters of different sources as we have here, we encounter two major hurdles to drawing decisive conclusions. The first is the issue of fair comparison since, as clearly shown in Table I, the literature does not always report all parameter values and thus it is not always possible to compare all aspects of different sources. Furthermore, as will be discussed in detail in section III, there exist flaws in the way that some parameters, particularly the brightness, are defined which raises further confusion when trying to draw comparisons.

The second issue is that for typical MRR there exists a trivariate trade-off between brightness, heralding efficiency, and purity. For example, increasing the spectral purity causes the heralding efficiency to decrease unless special design consider-

Reference	Source	B ₁ (MHz mW ⁻²)	B ₂ (MHz mW ⁻²)	B ₃ (MHz mW ⁻²)	H ₂ (%)	H ₃ (%)
[12] ^{a b}	MRR	204	-	0.0013	50	-
[13] ^b	MRR	-	124.93	-	50	-
[14] ^b	MRR	-	80	-	50	-
[15] ^b	MRR	149 ± 6	-	-	50	≈ 3.5
[16] ^c	ICR	4.4 ± 0.1	-	-	93.1 ± 3.1	6.4 ± 0.2
[17]	ICR	-	308	2.58	52.4 ± 3.0	-
[18] ^d	Multi-Mode Waveguide	0.89	0.89	0.06	91.0 ± 9.0	12.6 ± 0.2
[19]	Microdisk	-	136.98	-	-	-

TABLE II: A comparison between the brightness and heralding efficiencies of various literature HSPSs. Dashes represent when a particular parameter was not discussed

^a B₁ was determined using a theoretical model.

^b H₂ assumes maximum heralding efficiency at critical coupling.

^c H₂ is the average of separate signal and idler heralding efficiencies 92.1 ± 3.2 % and 94.0 ± 2.9 % respectively. H₃ is the average of separate signal and idler heralding efficiencies, 7.2 ± 0.2 % and 5.6 ± 0.2 % respectively.

^d A waveguide source is used, so B₁ and B₂ are equal.

ations are made to effectively decouple these parameters [16]. Increasing either the spectral purity or heralding efficiency also leads to reductions in brightness [43]. This is an aspect often overlooked in the literature, perhaps exacerbated by how it does not always report on all values thus obscuring evidence of trade-offs.

The ideal HSPS would maximise all parameters, and thus it is not enough to develop sources that focus on improving only the heralding efficiency or spectral purity. Instead, additional considerations must be made to reduce the impact of, or ideally overcome, trade-offs between parameters [31, 32, 44].

Outside of these issues, there are some additional intricacies to note about the literature. We can assume that, due to the multi-pair emission effect, all brightness-values are slightly over-inflated from the generation of multi-photon states. Brightness is usually measured at a low pump power such that four-wave mixing is the dominant process [28], or photon-number-resolving (PNR) or pseudo-PNR detectors are used to mitigate (although not completely eliminate) the multi-pair emission effect [45]. It is also worth noting that some literature divides the brightness by the pump profile linewidth for MRR or the bandwidth for waveguide sources to give units of HzW⁻²nm⁻¹ [19].

III. BRIGHTNESS AND HERALDING EFFICIENCY

A. Definitions

The brightness of a HSPS is defined as the photon pair generation rate per the square average power of the pump laser, per unit of time. Heralding efficiency is defined as the probability of a signal photon being present in the system, rather than lost to the environment, when an idler photon is detected. It is important to consider that at different points throughout the system, from source to detector, these parameters will decrease due to photon losses. The literature is not always clear with where exactly these parameters are measured in the system, which leads to inconsistencies when trying to compare the parameters of different sources.

This motivates the clear distinction of brightness and heralding efficiency parameters, defined with respect to where in the system they are measured. This is illustrated for the generic case of an MRR source with photons taken off-chip for detection in Figure 1. B₁ defines the effective brightness of the HSPS (also known as the intrinsic efficiency), B₂ is the corrected coincidence count rate at the point just after the nonlinear structure in which photon pairs are generated, and B₃ is the raw coincidence count rate recorded by the detectors. Analogous to this, H₁ is the intrinsic heralding efficiency of the

source (equal to unity by definition, and therefore shall be henceforth disregarded), H_2 is the corrected heralding efficiency, and H_3 is the raw heralding efficiency recorded by the detectors (also known as the Klyshko efficiency).

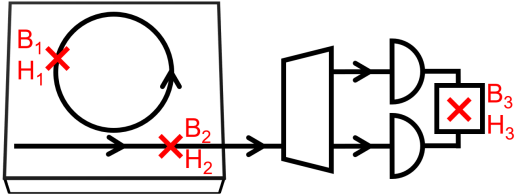


FIG. 1: The fundamental components of a typical MRR HSPS system, where the perspective rectangle represents an integrated chip, black arrows are the path of photons through waveguides or fiber, the trapezoid is a multiplexer that separates signal and idler photons, the semicircles are detectors, and the box containing B_3 and H_3 represents data collection and processing electronics.

B. Source Comparison

We will now expand upon Table I by considering these clearer definitions of brightness and heralding efficiency, illustrated by Table II. Here we can draw different conclusions about the comparison between sources; while the MRR in [15] has the highest value of B_1 , the ICR structure in [17] has the highest values of B_2 and B_3 . Furthermore, while the ICR structure in [16] has the highest value of H_2 , the waveguide source in [18] has the highest value of H_3 .

It is again apparent from Table II that there is an issue with fair comparison, since not all parameters are reported in the literature. However, it is important to note that some comparison tables in the literature make the mistake of comparing separate parameters, such as B_1 with B_2 , as if they had identical definitions [15, 16]. This highlights the necessity to clearly define whether a particular brightness value is B_1 , B_2 , or B_3 , which we speculate has not yet been attempted in the literature due to the focus on other parameters such as the purity of HSPSs (that said, [14] does consider pair generation rates at different points of the system, but does not elaborate on this in great detail).

Different processes of photon pair generation may have different units of brightness due to the number of pump photons involved which, for example, makes it not possible to compare B_1 and B_2 for HSPSs that utilise SFWM with those that use SPDC. However, it should be noted that an acceptable comparison could be made by using B_3 .

IV. OVERSIGHTS WITH BRIGHTNESS AND HERALDING EFFICIENCY

Using these new definitions of brightness and heralding efficiency as a foundation, we will now discuss several issues that often arise in the literature.

A. The Ideal Metric for Fair Comparison

When comparing different sources, H_2 is naturally the most valuable definition of heralding efficiency (and is indeed the one considered in Table I), as it disregards losses from any other component than the source itself. Meanwhile H_3 is more useful when considering the performance of the HSPS system as a whole. H_3 can be calculated by dividing the detector coincidence count rate ($R_{s,i}$) by the signal photon count rate, R_s [46, 47]. H_2 can then be estimated from H_3 by considering sources of loss within the system.

The current methods used for estimating brightness parameters have a great impact on their usefulness for comparing different sources, with the flaws in these methods forming the bulk of the remainder of this work. B_3 can be determined by measuring $R_{s,i}$ of the detectors for a given average pump power, and dividing by the square of the power. B_2 can then be estimated from B_3 by again accounting for losses between the source and detectors. This method for determining B_2 will be referred to as the point-based method. B_1 can be calculated by considering the dependence of $R_{s,i}$ on the average pump power using equations [48]. The count rate recorded for signal, R_s , and idler, R_i , photons and $R_{s,i}$ can be related to B_1 , γ_{eff} , using equations 1, 2, and 3.

$$R_s = (\eta_s \gamma_{eff}) P_{avg}^2 + \beta_s P_{avg} + DC_s \quad (1)$$

$$R_i = (\eta_i \gamma_{eff}) P_{avg}^2 + \beta_i P_{avg} + DC_i \quad (2)$$

$$R_{s,i} = (\eta_i \eta_s \gamma_{eff}) P_{avg}^2 + ACC \quad (3)$$

Here η represents detection efficiency, β is the noise proportional to pump power (such as the pump leakage), and DC and ACC are the dark counts and accidentals [25]. Experimental measurements of these count rates for varying P_{avg} can be fit to the equations to determine γ_{eff} [48], providing an accurate estimate of B_1 that we will refer to as the equation-based method.

Similarly to H_2 , B_2 is, in theory, the most valuable definition of brightness when comparing sources, because it isolates the performance of the source from the performance of other system elements. However, in Table I B_1 is considered instead of B_2 as it is determined using the far more accurate, although less-trivial, equation-based method. This improvement makes B_1 the most accurate definition of brightness currently for comparing sources, restricting B_2 to being most useful for estimating of the source output, while B_3 is most useful for considering the output from the system as a whole.

Unfortunately, measurements of B_2 are noticeably more common in the literature, likely due to their relative simplicity compared to measuring B_1 . Additionally, while useful for comparing sources, B_1 does not give an accurate estimate of the output that can be expected from a given source. This is because, while B_1 can be optimised by operating in the critical coupling regime, B_2 is optimised when operating in a somewhat over-coupled regime [43].

It may be possible to overcome this challenge by determining B_2 from the more accurate, equation-based method. This would require measuring B_1 and then considering losses. However, this would require a very good understanding of various factors such as, in the case of MRR, the quality factor and coupling regime in order to accurately estimate the amount of light that successfully escapes the resonator. In comparison, this would be far simpler in the case of waveguide sources, where B_1 and B_2 can be considered to be approximately equal if one ignores propagation losses within the generation-region, due to low loss or short generation waveguides. Figure 2 compares how B_1 and B_2 are defined for MRR and waveguide sources. The non-trivial calculations required to convert B_1 to B_2 opens up many possible sources of error, and to our knowledge

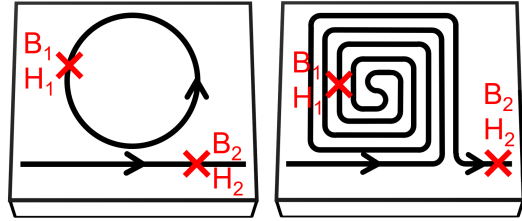


FIG. 2: How B_1 and B_2 are defined for a MRR (left) and waveguide source (right).

this has not yet been attempted in the literature (indeed, all sources discussed in Table II determine B_2 using the point-based method). Otherwise, if B_2 could be determined readily and accurately using the equation-based method, it could be considered as the definitive brightness parameter for comparing sources.

B. Dependence of Brightness on Repetition Rate

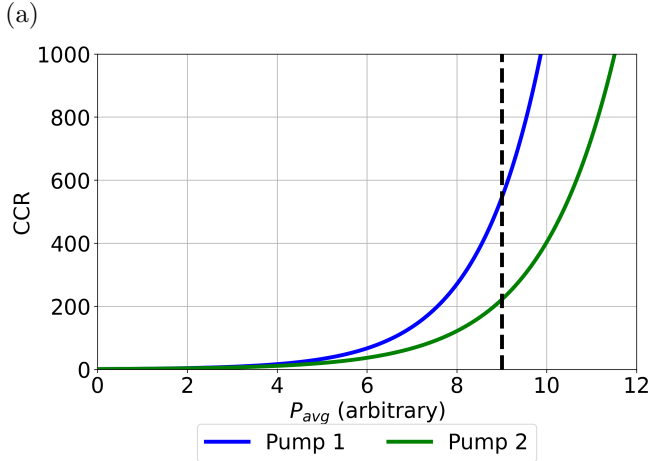
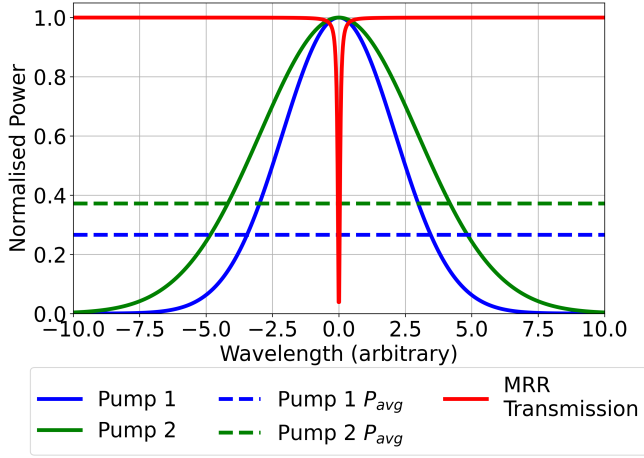
It makes intuitive sense that a pulsed pump laser with a higher repetition rate, R , will yield a higher value of brightness, which can be understood with equation 4.

$$\bar{n} = \frac{\gamma_{eff} P_{avg}^2}{R} \quad (4)$$

Here \bar{n} is the average number of photon pairs generated per pulse, and we can see that the dependence on the repetition rate can be removed from the brightness by simply multiplying brightness by R . This was first suggested in [16] and gives the brightness units of energy (pJ^{-2}) rather than power. In the case of the brightness parameters from Table II, this would not significantly impact the comparison of results as they all have roughly similar repetition rates. In the case where a continuous-wave (CW) laser is used, since there is no repetition rate, the only intuitive parameter to multiply the brightness by would be the detector integration time. This is an arguably arbitrary choice, and thus these units are less useful.

C. Inaccuracies due to Pump Bandwidth

When calculating the brightness of an MRR, it would be more accurate to consider the average



(b)

FIG. 3: Theoretical examples to illustrate that (a) two pump pulses with significantly different values of P_{avg} may still have an almost identical overlap with the MRR transmission, and (b) how these differences might influence how brightness is determined when plotting $R_{s,i}$ against P_{avg} .

pump power within the resonator rather than the average pump power from the laser. This is not an issue for waveguide sources, since the phase matching condition (unless very narrow) results in the majority of pump power being used to produce photon pairs. However, for MRR, the phase matching condition means the resonator can only absorb a fraction of the pump light.

This concept is illustrated in Figure 3a, where two different Gaussian pump pulses have a very similar overlap with the Lorentzian MRR transmission, but very different values of P_{avg} . This means that both pump pulses couple almost equally to the MRR and hence generate similar numbers of photon pairs,

but the differing values of P_{avg} result in a large erroneous difference in the value of B_1 between the two sources. This is illustrated by Figure 3b, where $R_{s,i}$ for each of the pulse pulses have a large discrepancy between them for a given value of P_{avg} (represented by the black dashed line).

To our knowledge, currently this consideration has not yet been made in the literature, and presents a serious flaw in the way brightness is determined for MRR sources. To rectify this, future measurements should consider the average pump power within the ring, rather than the average pump power output from the laser.

D. Inaccuracies due to non-Unity Spectral Purity

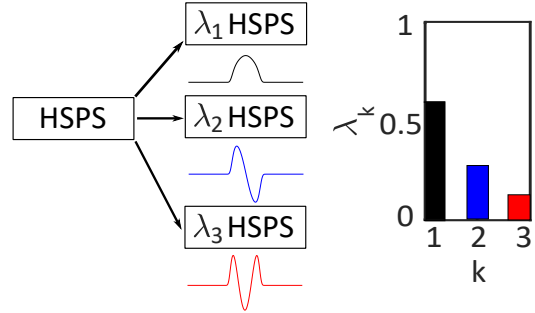


FIG. 4: How one HSPS can effectively be split into multiple HSPSs for different Schmidt modes, λ_k . Here the first three Schmidt modes are illustrated as an example.

While the multi-pair emission effect can be considered negligible, such that the photon number purity of the HSPS has an insignificant effect on brightness, it is not possible to do so with the spectral purity. When the spectral purity is non-unity, the HSPS will emit in multiple Schmidt modes, as illustrated in Figure 4. As a result, the HSPS can be considered as multiple separate HSPSs for each Schmidt mode, each source will have ideal spectral purity but brightness will be split amongst them. Thus, brightness should ideally be calculated per Schmidt mode in the case where spectral purity is not unity.

V. OUTLOOK

In conclusion, we have analysed the state-of-the-art in HSPS research, comparing the parameters of different sources and suggesting ways that future research could be improved. Moving forwards, particular care should be taken to clearly define the brightness and heralding efficiency of HSPSs based on where in the system they are considered. The way brightness is measured could be further improved by removing the dependence of brightness on repetition rate and, in the case of MRR, by using the average pump power within the resonator itself. It is also important to consider trade-offs that exist between HSPS parameters, particularly the brightness, heralding efficiency, and purity.

VI. ACKNOWLEDGEMENTS

The authors acknowledge funding and support from the Engineering and Physical Science Research Council (EPSRC) Hibbert Scholarship, EP/SO23607/1, and the EPSRC Quantum Communications Hubs, EP/M013472/1 and EP/T001011/1.

-
- [1] J. O’Brien, A. Furusawa, and J. Vučković, Photonic quantum technologies, *Nat. Photon.* **3** (2009).
- [2] S. Bartolucci *et al.*, Fusion-based quantum computation, *Nat. Commun.* **14** (2023).
- [3] S. Takeda and A. Furusawa, Toward large-scale fault-tolerant universal photonic quantum computing, *APL Photon.* **4** (2019).
- [4] S. Pirandola *et al.*, Advances in Quantum Cryptography, *Adv. Opt. Photon.* **12** (2020).
- [5] C. Lu *et al.*, Micius quantum experiments in space, *Rev. Mod. Phys.* **94** (2022).
- [6] D. Rauch *et al.*, Cosmic Bell Test Using Random Measurement Settings from High-Redshift Quasars, *Phys. Rev. Lett.* **121** (2018).
- [7] M. Mohageg *et al.*, The deep space quantum link: prospective fundamental physics experiments using long-baseline quantum optics, *EPJ Quantum Technol.* **9** (2022).
- [8] R. Horn *et al.*, Monolithic Source of Photon Pairs, *Phys. Rev. Lett.* **108** (2012).
- [9] N. Matsuda *et al.*, A monolithically integrated polarization entangled photon pair source on a silicon chip, *Sci. Rep.* **2** (2012).
- [10] J. Silverstone *et al.*, Silicon Quantum Photonics, *IEEE J. Sel. Top. Quantum Electron.* **22** (2016).
- [11] K. Alexander *et al.*, A manufacturable platform for photonic quantum computing, arXiv:2404.17570 [quant-ph] (2024).
- [12] J. Silverstone *et al.*, Qubit entanglement between ring-resonator photon-pair sources on a silicon chip, *Nat. Commun.* **6** (2015).
- [13] R. Wakabayashi *et al.*, Time-bin entangled photon pair generation from Si micro-ring resonator, *Opt. Express* **23** (2015).
- [14] M. Savanier, R. Kumar, and S. Mookherjea, Optimizing photon-pair generation electronically using a p-i-n diode incorporated in a silicon microring resonator, *Appl. Phys. Lett.* **107** (2015).
- [15] C. Ma *et al.*, Silicon photonic entangled photon-pair and heralded single photon generation with CAR $>12,000$ and $g^{(2)}(0) < 0.006$, *Opt. Express* **25** (2017).
- [16] B. Burrige *et al.*, Integrate and scale: a source of spectrally separable photon pairs, *Optica* **10** (2023).
- [17] Y. Liu *et al.*, High-spectral-purity photon generation from a dual-interferometer-coupled silicon microring, *Opt. Lett.* **45** (2020).
- [18] S. Paesani *et al.*, Near-ideal spontaneous photon sources in silicon quantum photonics, *Nat. Commun.* **11** (2020).
- [19] W. Jiang *et al.*, Silicon-chip source of bright photon pairs, *Opt. Express* **23** (2015).
- [20] L. Helt *et al.*, Spontaneous four-wave mixing in microring resonators, *Opt. Lett.* **35** (2010).
- [21] T. Rudolph, Why I am optimistic about the silicon-photon route to quantum computing, *APL Photon.* **2** (2017).
- [22] S. Li *et al.*, Scalable Deterministic Integration of Two Quantum Dots into an On-Chip Quantum Circuit, *ACS Photonics* **10** (2023).
- [23] F. Kaneda and P. Kwiat, High-efficiency single-photon generation via large-scale active time multiplexing, *Sci. Adv.* **5** (2019).
- [24] D. DiVincenzo, The Physical Implementation of Quantum Computation, *Fortschr. Phys.* **48** (2000).
- [25] I. Faruque *et al.*, On-chip quantum interference with heralded photons from two independent micro-ring resonator sources in silicon photonics, *Opt. Express* **26** (2018).
- [26] I. Faruque *et al.*, Estimating the Indistinguishability of Heralded Single Photons Using Second-Order Correlation, *Phys. Rev. Appl.* **12** (2019).
- [27] J. Spring *et al.*, Chip-based array of near-identical, pure, heralded single-photon sources, *Optica* **4** (2017).
- [28] D. Llewellyn *et al.*, Chip-to-chip quantum teleportation and multi-photon entanglement in silicon, *Nat. Phys.* **16** (2020).
- [29] D. Zhu *et al.*, Resolving Photon Numbers Using a Superconducting Nanowire with Impedance-Matching Taper, *Nano Lett.* **20** (2020).
- [30] Z. Vernon *et al.*, Truly unentangled photon pairs without spectral filtering, *Opt. Lett.* **42** (2017).
- [31] B. Burrige *et al.*, High spectro-temporal purity single-photons from silicon micro-racetrack resonators using a dual-pulse configuration, *Opt. Lett.* **45** (2020).
- [32] J. Christensen *et al.*, Engineering spectrally unentangled photon pairs from nonlinear microring resonators by pump manipulation, *Opt. Lett.* **43** (2018).
- [33] E. Meyer-Scott *et al.*, Single-photon sources: Approaching the ideal through multiplexing, *Rev. Sci. Instrum.* **91** (2020).
- [34] F. Kaneda *et al.*, Heralded single-photon source utilizing highly nondegenerate, spectrally factorable spontaneous parametric downconversion, *Opt. Express* **24** (2016).
- [35] Y. Cao *et al.*, Bell Test over Extremely High-Loss Channels: Towards Distributing Entangled Photon Pairs between Earth and the Moon, *Phys. Rev. Lett.* **120** (2018).
- [36] M. Liu and H. Lim, Efficient heralding of O-band passively spatial-multiplexed photons for noise-tolerant quantum key distribution, *Opt. Express* **22** (2014).
- [37] J. Yin *et al.*, Entanglement-based secure quantum cryptography over 1,120 kilometres, *Nature* **582**

- (2020).
- [38] F. Steinlechner *et al.*, A high-brightness source of polarization-entangled photons optimized for applications in free space, *Opt. Express* **20** (2012).
 - [39] H. A *et al.*, Low Loss, Large Bandwidth Fiber-Chip Edge Couplers Based on Silicon-on-Insulator Platform, *J. Lightwave Technol.* **38** (2020).
 - [40] C. Husko *et al.*, Multi-photon absorption limits to heralded single photon sources, *Sci. Rep.* **3** (2013).
 - [41] C. Zhang *et al.*, Spontaneous Parametric Down-Conversion Sources for Multiphoton Experiments, *Adv. Quantum Technol.* **4** (2021).
 - [42] R. Savanier, M. Kumar and S. Mookherjea, Photon pair generation from compact silicon microring resonators using microwatt-level pump powers, *Opt. Express* **24** (2016).
 - [43] Z. Vernon, M. Liscidini, and J. Sipe, No free lunch: the trade-off between heralding rate and efficiency in microresonator-based heralded single photon sources, *Opt. Lett.* **41** (2016).
 - [44] L. Rodda *et al.*, Effect on spectral purity due to on-chip temporal manipulation of the pump, arXiv:2404.03986 [quant-ph] (2024).
 - [45] G. Moody *et al.*, 2022 Roadmap on integrated quantum photonics, *J. Phys. Photonics* **4** (2022).
 - [46] E. Meyer-Scott *et al.*, High-performance source of spectrally pure, polarization entangled photon pairs based on hybrid integrated-bulk optics, *Opt. Express* **26** (2018).
 - [47] L. Xiyuan *et al.*, Heralding single photons from a high-Q silicon microdisk, *Optica* **3** (2016).
 - [48] D. Bonneau, J. Silverstone, and M. Thompson, Silicon Photonics III Systems and Applications, Chapter 2 Silicon Quantum Photonics (Springer, 2016) pp. 41–82.